International Journal of Fluid Power 14 (2013) No. 1 pp. 37-45

PRESSURE ESTIMATION-BASED ROBUST FORCE CONTROL OF PNEUMATIC ACTUATORS

Tad Driver and Xiangrong Shen

The Department of Mechanical Engineering at The University of Alabama,
290 Hardaway Hall, Box 870276, Tuscaloosa, AL 35487-0276, USA
xshen@eng.ua.edu

Abstract

Pneumatic actuators enjoy a number of unique advantages, such as high power density and low cost, in comparison with the widely used electromagnetic actuators. In this paper, a new force control approach is presented for pneumatic actuation systems, with the objective of providing robust control performance while eliminating the need for pressure sensors to reduce the cost and complexity of the system. To achieve this goal, a unique pressure estimation algorithm is developed to provide the required chamber pressure information. This pressure estimation algorithm is formulated according to two simultaneous conditions, established based on the measured actuation force and the average air pressure in the actuator. Utilizing these conditions, the chamber pressures can be calculated through simple algebraic equations instead of complex pressure observers. For the force controller design, the dynamic model of the entire system is developed, and the standard sliding mode control approach is applied to obtain a robust control law. In the experiments, the hypothesis of constant average pressure was verified. Also, the pressure estimation algorithm and the corresponding robust control approach were implemented, and the effectiveness demonstrated by the sinusoidal and square-wave force tracking.

Keywords: pneumatics, pneumatic control, pressure estimation, robust control.

1 Introduction

For robotic actuators, especially those used in mobile and portable robotic systems, a fundamental requirement is high force and power density, i.e., generating large force and power output with low weight and small volume. The pneumatic actuator, with its significantly improved energetics in comparison with the traditional electromagnetic-type actuator (Kuribayashi 1992), poses an attractive choice for such systems. Additionally, pneumatic actuators usually are less expensive, and they are suitable for the use in clean environments. The schematic of a typical pneumatic system is shown in Fig. 1. In such a system, a four-way proportional servo valve regulates the pressurizing and exhausting mass flows into or out of the two chambers of the pneumatic cylinder, and thus controls the force or power output to the load. Note that, in a large number of robotic systems, the need for a natural interaction with the environment requires the actuator to be treated as a source of actuation force, i.e., a force generator (Kazerooni 2005). As such, the capability of precisely modulating the output force in the presence of external disturbance makes a significant research topic in the robotic application of pneumatic actuators.

Due to the multiple nonlinearities involved in a pneumatic actuation system, the control of such systems poses a significant challenge. A considerable amount of research has been conducted on this topic. In 1950's, Shearer studied the thermodynamic and flow dynamic processes in the pneumatic systems, with the results forming a basis for the subsequent modeling and control works (1956a, 1956b, 1957). For the effective control of pneumatic systems, a variety of control approaches have been attempted, including the linear controller developed by Ben-Dov and Salcudean (1995), the adaptive position and force controller by Bobrow and Jabbari (1991) and McDonell and Bobrow (1993), the backstepping controller by Smaoui et al. (2006), the twisting algorithm by Taleb et al. (2012), and the sliding mode controllers by Arun et al. (1994), Tang and Walker (1995), Richer and Hurmuzlu (2000a, 2000b), Smaoui et al. (2008), Girin et al. (2009), Bregeault et al. (2010) and Plestan et al. (2012).

This manuscript was received on 14 August 2012 and was accepted after revision for publication on 12 January 2013

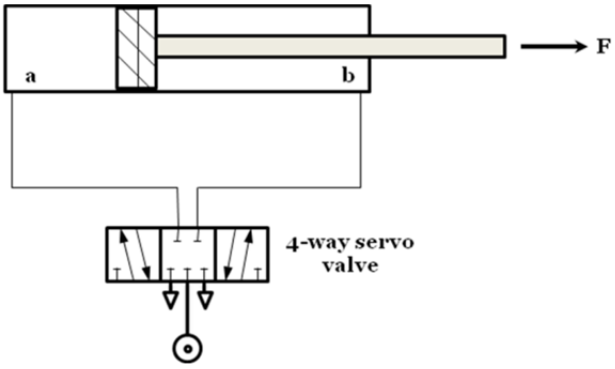

Fig. 1: *Schematic of the pneumatic actuation system*

Note that, pneumatic systems involve significant nonlinearity in the dynamic model. As such, model-based nonlinear control approaches, such as the sliding mode control, are usually more effective than the traditional linear control approaches. By incorporating the model information into the controller design, model-based approaches have a strong capability in addressing the nonlinearities in the system and providing good control performance. However, the implementation of a model-based controller usually requires full-state feedback, and thus poses extra sensing and instrumentation requirements. Especially for the feedback of the required pressure signals, pressure sensors need to be incorporated into the pneumatic actuation system. However, a pressure sensor requires special signal conditioning and acquisition circuitry, and incurs extra cost. In addition, a single pneumatic actuator requires two pressure sensors for the control purpose, further exacerbating the problem.

Because of the apparent benefits of eliminating pressure sensors in the pneumatic control systems, researchers have investigated the possibility of providing the required pressure information without using pressure sensors. Pandian et al. (1997) presented two methods for pressure observation: the first method is a continuous gain observer, in which the pressure is measured in one chamber and observed in the other, thus reducing the number of pressure sensors from two to one; the second method is a sliding mode pressure observer, in which the error in the pressure observation is treated as a disturbance. Bigras and Khayati (2002) presented a pressure observer for pneumatic systems with connection ports generating significant flow restriction. In their design, the observer utilizes the measured pressure outside the cylinder as one of the inputs, and thus does not totally eliminate the need for pressure sensors. Similarly, Girin et al. (2006) presented high gain and sliding mode observers that also use a measured pressure signal (in one of the chambers) as an input. In addition, Gulati and Barth (2009) presented a globally stable Lyapunov-based pressure observer, in which the Lyapunov function is defined based on the energy stored in the two chambers of the actuator. Note that the approaches described above are all based on the observer theory, which requires continuous integration in the operation. As such, these approaches may pose a higher requirement for computational capability in the implementation. More importantly, according to a nonlinear observability analysis conducted by Wu et al. (2004), the pneumatic system loses local observability at several points in the state space, posing a potential concern for the effectiveness of such pressure observers.

Unlike the observer-based approaches described above, the method presented in this paper aims at obtaining the required pressure information from a set of simple algebraic equations. Specifically, with the actuation force measurement in a typical force-controlled pneumatic system, an algebraic equation can be established based on the pressure-force relationship. Additionally, the second algebraic equation can be established based on the assumption of nearly constant average pressure in the actuator, and the value of the average pressure can be obtained through the mass flow balance of the actuator. The two equations provide sufficient information for the estimation of the two chamber pressures, which can be utilized for the implementation of the robust force control algorithm. The paper is organized as follows: Section 2 presents the pressure estimation algorithm; Section 3 presents the derivation of the dynamic model of the force-controlled pneumatic system; Section 4 presents the model-based robust control algorithm for the tracking of the desired actuation force; Section 5 presents the experimental results; and Section 6 contains the conclusions of this paper.

2 Pressure Estimation Algorithm

For a typical double-acting pneumatic actuator shown in Fig. 1, the actuation force can be expressed as a function of the gas pressures in the actuator chambers:

$$F = P_a A_a - P_b A_b - P_{atm} A_r \tag{1}$$

where P_a and P_b are the absolute pressures in the chambers *a* and *b*, respectively; P_{atm} is the atmosphere pressure; A_a and A_b are the effective areas of each side of the piston; and A_r is the cross-sectional area of the piston rod. Here the internal friction is neglected due to the significantly smaller magnitude than the forces generated by air pressure. Note that Eqn. (1) not only serves as a description of the dynamic process, but can also be used for the estimation of the chamber pressures, utilizing the measured actuation force as the input. From a mathematic perspective, however, an additional equation is needed to completely determine the two chamber pressures. In the proposed approach, such equation can be obtained through an average pressure in the entire actuator, which, in turn, can be derived from the mass flow balance through the actuator. Specifically, because of the four-way valve used in the pneumatic system, the pressurizing of one actuator chamber is always accompanied by the depressurizing of the other chamber. As such, it can be deduced that, in a reciprocating motion, after the system reaches the steady state, the average pressure in the actuator will remain close to a constant value with only small fluctuation. The experimental verification of this hypothesis

is presented later in the section of Experimental Results. Based on this hypothesis, the second condition in the pressure estimation can be expressed by the following equation:

$$P_{\text{ave}} = \frac{P_{\text{a}}V_{\text{a}} + P_{\text{b}}V_{\text{b}}}{V_{\text{a}} + V_{\text{b}}} \approx \text{constant} \tag{2}$$

Note that the averaging of the chamber pressures is conducted based on the corresponding volumes at the current state. Note also that the value of the average pressure is required for the implementation of this equation in the pressure estimation. Here this value is obtained by studying the inflow-outflow balance of the actuator (Fig. 2). Specifically, after the system reaches the steady state, the air mass stored in the actuator is negligible in comparison with the cumulative mass flow into or out of the actuator. As such, the cumulative inflow and outflow are in total balance, as expressed by the following equation:

$$m_{\text{in}} = m_{\text{out}} \tag{3}$$

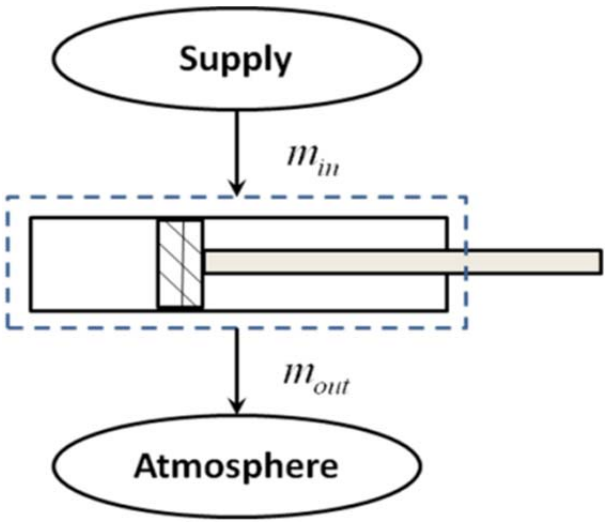

Fig. 2: *The balance of the inflow and outflow: $m_{in} = m_{out}$*

Therefore, the average inflow and outflow rates are also in balance:

$$\dot{m}_{\text{in,ave}} = \dot{m}_{\text{out,ave}} \tag{4}$$

The above equation can be further expanded by incorporating the relationship between the mass flow rate and the corresponding valve opening area. Modeling the flow through the valve as a flow of an ideal gas undergoing an isentropic process, the mass flow rate can be expressed as a function of the corresponding valve area (Blackburn et al. 1960):

$$\dot{m}(P_{\text{u}}, P_{\text{d}}) = A_{\text{v,e}}\Psi(P_{\text{u}}, P_{\text{d}}) \tag{5}$$

where

$$\Psi(P_{\text{u}}, P_{\text{d}}) = \begin{cases} \sqrt{\dfrac{\gamma}{RT}\left(\dfrac{2}{\gamma+1}\right)^{\frac{(\gamma+1)}{(\gamma-1)}}} C_{\text{f}}P_{\text{u}} \\ \qquad \text{if} \quad \dfrac{P_{\text{d}}}{P_{\text{u}}} \le C_{\text{r}} \ \text{(choked)} \\ \sqrt{\dfrac{2\gamma}{RT(\gamma-1)}}\sqrt{1-\left(\dfrac{P_{\text{d}}}{P_{\text{u}}}\right)^{\frac{(\gamma-1)}{\gamma}}}\left(\dfrac{P_{\text{d}}}{P_{\text{u}}}\right)^{\frac{1}{\gamma}} C_{\text{f}}P_{\text{u}} \\ \qquad \text{otherwise (unchoked)} \end{cases} \tag{6}$$

and $A_{\text{v,e}}$ is the effective valve opening area, P_{u} and P_{d} are the upstream and downstream pressures, respectively, R is the universal gas constant, T is the gas temperature, C_{f} is the discharge coefficient of the valve (which accounts for irreversible flow conditions), and C_r is the pressure ratio that divides the flow regimes into unchoked (sub-sonic) and choked (sonic) flow through the orifice. Substituting (5) into (4),

$$A_{\text{v,in}}\Psi(P_{\text{s}}, P_{\text{ave}}) = A_{\text{v,out}}\Psi(P_{\text{ave}}, P_{\text{atm}}) \tag{7}$$

where $A_{\text{v,in}}$ and $A_{\text{v,out}}$ are the average valve areas for pressurizing and depressurizing, respectively; P_{s} is the supply pressure; P_{atm} is the atmosphere pressure; and P_{ave} is the average pressure in the actuator chambers. Note that, with the use of the four-way valve in the typical pneumatic system (Fig. 1), the average pressurizing valve area is always equal to the average exhausting valve area:

$$A_{\text{v,in}} = A_{\text{v,out}} \tag{8}$$

Substituting (8) into (7), the following equation can be obtained:

$$\Psi(P_{\text{s}}, P_{\text{ave}}) = \Psi(P_{\text{ave}}, P_{\text{atm}}) \tag{9}$$

which can be used for the estimation of the average pressure. As shown in Fig. 3, with the supply pressure fixed, both the left-hand side and right-hand side can be expressed as functions of the average pressure P_{ave}, and thus the value of P_{ave} is essentially determined by the intersection of two curves, as indicated by (9).

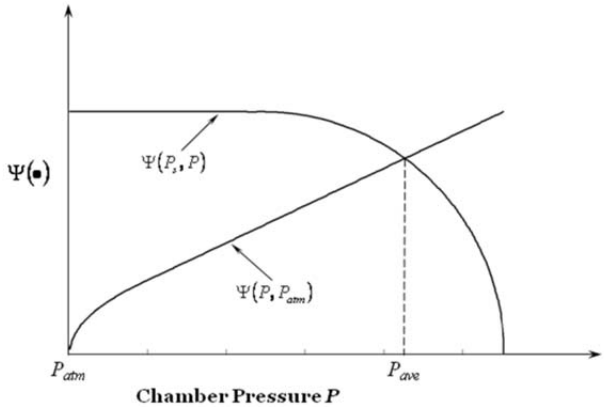

Fig. 3: *Determination of the average pressure through the balance of the inflow and outflow*

With the average pressure calculated from (9), Eq. (1) and (2) can be combined to solve for the chamber pressures as the estimation of the pressure states. In Eq. (2), the volume in each chamber is a geometric function of piston displacement x (with the mid-stroke position

as the origin), given by

$$V_{\mathrm{a}} = A_{\mathrm{a}}\left(\frac{L}{2}+x\right) \tag{10}$$

$$V_{\mathrm{b}} = A_{\mathrm{b}}\left(\frac{L}{2}-x\right) \tag{11}$$

where L is the length of the actuator. Substituting (10) and (11) into (2) yields

$$P_{\mathrm{ave}} = \frac{P_{\mathrm{a}}A_{\mathrm{a}}\left(\frac{L}{2}+x\right)+P_{\mathrm{b}}A_{\mathrm{b}}\left(\frac{L}{2}-x\right)}{A_{\mathrm{a}}\left(\frac{L}{2}+x\right)+A_{\mathrm{b}}\left(\frac{L}{2}-x\right)} \tag{12}$$

Combining (12) with (1), the estimated pressures can be expressed by the following equations:

$$P_{\mathrm{a}} = \frac{1}{A_{\mathrm{a}}L}\left[\begin{array}{l} P_{\mathrm{ave}}A_{\mathrm{a}}\left(\frac{L}{2}+x\right)+P_{\mathrm{ave}}A_{\mathrm{b}}\left(\frac{L}{2}-x\right)+ \\ \left(F+P_{\mathrm{atm}}A_{\mathrm{r}}\right)\left(\frac{L}{2}-x\right) \end{array}\right] \tag{13}$$

$$P_{\mathrm{b}} = \frac{1}{A_{\mathrm{b}}L}\left[\begin{array}{l} P_{\mathrm{ave}}A_{\mathrm{a}}\left(\frac{L}{2}+x\right)+P_{\mathrm{ave}}A_{\mathrm{b}}\left(\frac{L}{2}-x\right)- \\ \left(F+P_{\mathrm{atm}}A_{\mathrm{r}}\right)\left(\frac{L}{2}+x\right) \end{array}\right] \tag{14}$$

3 Modeling the Force-Controlled Pneumatic System

With the pressure estimation presented in the previous section, a model-based robust control approach can be developed and implemented for the highly nonlinear pneumatic system. In the section, a complete dynamic model, from the valve command (opening area) as the input to the actuation force as the output, will be presented as a basis for the following robust controller design.

The derivation of the dynamic model starts from the differentiation of the expression for the actuation force (1):

$$\dot{F} = \dot{P}_{\mathrm{a}}A_{\mathrm{a}} - \dot{P}_{\mathrm{b}}A_{\mathrm{b}} \tag{15}$$

Assuming air is an ideal gas undergoing an isothermal process, the rate of change of the pressure inside each chamber of the cylinder can be expressed as:

$$\dot{P}_{(\mathrm{a,b})} = \frac{RT}{V_{(\mathrm{a,b})}}\dot{m}_{(\mathrm{a,b})} - \frac{P_{(\mathrm{a,b})}}{V_{(\mathrm{a,b})}}\dot{V}_{(\mathrm{a,b})} \tag{16}$$

where $\dot{m}_{(\mathrm{a,b})}$ is the mass flow rate into (positive) and out of (negative) each side of the cylinder, and $V_{(\mathrm{a,b})}$ is the volume of each cylinder chamber. Here the rates of change of the chamber volumes can be obtained by differentiating (10) and (11):

$$\dot{V}_{\mathrm{a}} = \dot{x}A_{\mathrm{a}} \tag{17}$$

$$\dot{V}_{\mathrm{b}} = -\dot{x}A_{\mathrm{b}} \tag{18}$$

where $\dot{x}$ is the velocity of the piston. The mass flow rates $\dot{m}_{(\mathrm{a,b})}$ can be expressed as functions of the corresponding valve opening areas according to (5). Note that, with the use of a single four-way spool valve in the system, one of the two chambers is connected to the supply while the other is connected to the exhaust (atmosphere). As such, the effective valve opening area to the two chambers can be related according to the following equation:

$$A_{\mathrm{v,a}} = -A_{\mathrm{v,b}} = A_{\mathrm{v}} \tag{19}$$

where A_{v} is the valve command. As indicated by this equation, a positive valve command corresponds to pressurizing Chamber *a* and exhausting Chamber *b*, while a negative command corresponds to the opposite. The corresponding equations for $\dot{m}_{\mathrm{a}}$ and $\dot{m}_{\mathrm{b}}$ are:

$$\dot{m}_{\mathrm{a}} = A_{\mathrm{v}}\Psi_{\mathrm{a}} \tag{20}$$

where

$$\Psi_{\mathrm{a}} = \begin{cases} \Psi(P_{\mathrm{s}},P_{\mathrm{a}}) & \textit{if } A_{\mathrm{v}} \geq 0 \\ \Psi(P_{\mathrm{a}},P_{\mathrm{atm}}) & \textit{if } A_{\mathrm{v}} < 0 \end{cases} \tag{21}$$

and

$$\dot{m}_{\mathrm{b}} = -A_{\mathrm{v}}\Psi_{\mathrm{b}} \tag{22}$$

where

$$\Psi_{\mathrm{b}} = \begin{cases} \Psi(P_{\mathrm{b}},P_{\mathrm{atm}}) & \textit{if } A_{\mathrm{v}} \geq 0 \\ \Psi(P_{\mathrm{s}},P_{\mathrm{b}}) & \textit{if } A_{\mathrm{v}} < 0 \end{cases} \tag{23}$$

Substituting (10) through (11), (16) through (18), (20), and (22) into (15), the following equation can be obtained:

$$\dot{F} = \left(\frac{RT}{\frac{L}{2}+x}\Psi_{\mathrm{a}} + \frac{RT}{\frac{L}{2}-x}\Psi_{\mathrm{b}}\right)A_{\mathrm{v}} - \left(\frac{P_{\mathrm{a}}A_{\mathrm{a}}}{\frac{L}{2}+x} + \frac{P_{\mathrm{b}}A_{\mathrm{b}}}{\frac{L}{2}-x}\right)\dot{x} \tag{24}$$

This equation can be further converted into the companion form to facilitate the following controller design:

$$\dot{F} = f(\mathbf{x}) + p(\mathbf{x})A_{\mathrm{v}} \tag{25}$$

where

$$f(\mathbf{x}) = -\left(\frac{P_{\mathrm{a}}A_{\mathrm{a}}}{\frac{L}{2}+x} + \frac{P_{\mathrm{b}}A_{\mathrm{b}}}{\frac{L}{2}-x}\right)\dot{x} \tag{26}$$

$$p(\mathbf{x}) = \frac{RT}{\frac{L}{2}+x}\Psi_{\mathrm{a}} + \frac{RT}{\frac{L}{2}-x}\Psi_{\mathrm{b}} \tag{27}$$

And the state vector $\mathbf{x}$ consists of the pressure in each side of the actuator, along with the displacement and velocity of the piston:

$$\mathbf{x} = \begin{bmatrix} x & \dot{x} & P_{\mathrm{a}} & P_{\mathrm{b}} \end{bmatrix}^{\mathrm{T}} \tag{28}$$

4 Robust Force Controller Design

Based on the nonlinear model developed in the previous section, the standard sliding mode control ap-

proach is applied to obtain a robust force controller (Slotine and Li 1991). Sliding mode control is selected to maintain the control stability and provide a consistent control performance in the existence of model uncertainties and disturbances. First, since the system dynamic model (25) is first-order, a sliding surface $S(t)$ is selected as:

$$s = F - F_{\mathrm{d}} = 0 \tag{29}$$

where F_{d} is the desired actuation force. A robust control law can be obtained by combining an equivalent control component $A_{\mathrm{v,eq}}$ with a robustness control component$A_{\mathrm{v,rb}}$:

$$A_{\mathrm{v}} = A_{\mathrm{v,eq}} + A \tag{30}$$

The equivalent control component $A_{\mathrm{v,qe}}$ is used to achieve the desired motion on the sliding surface

$$\dot{s} = 0 \tag{31}$$

which gives the following expression:

$$A_{\mathrm{v,eq}} = \frac{\dot{F}_{\mathrm{d}} - \hat{f}(\mathbf{x})}{\hat{p}(\mathbf{x})} \tag{32}$$

where $\hat{f}(\mathbf{x})$ and $\hat{p}(\mathbf{x})$ are the nominal values of $f(\mathbf{x})$ and $p(\mathbf{x})$, respectively. The robustness component $A_{\mathrm{v,rb}}$ is used to accommodate the model uncertainties and disturbances. Specifically, assume that the uncertainty of the model parameters is bounded, as expressed by the following conditions:

$$\beta^{-1} \le \frac{p(\mathbf{x})}{\hat{p}(\mathbf{x})} \le \beta \tag{33}$$

and

$$\left| f(\mathbf{x}) - \hat{f}(\mathbf{x}) \right| \le F(\mathbf{x}) \tag{34}$$

where β is the gain margin of the controller design, and $F(\mathbf{x})$ is a boundary function that limits the uncertainty associated with $f(\mathbf{x})$. To satisfy the sliding condition

$$\frac{1}{2}\frac{d}{dt}s^2 \le -\eta|s| \tag{35}$$

(η is the rate of converging to the sliding surface) the robustness component $A_{\mathrm{v,rb}}$ is chosen as

$$A_{\mathrm{v,rb}} = -\frac{G}{\hat{p}(\mathbf{x})} \cdot \mathrm{sgn}(s) \tag{36}$$

where the robustness gain G is chosen such that

$$G \ge \beta\left(F(\mathbf{x}) + \eta\right) + \left(\beta - 1\right) \cdot \left| \hat{p}(\mathbf{x}) \cdot A_{\mathrm{v,eq}} \right| \tag{37}$$

In the implementation of the sliding mode controller, the robustness component (36) is slightly modified to incorporate a thin boundary layer neighboring the sliding surface, with the purpose of eliminating chattering and smoothing out the control discontinuities:

$$A_{\mathrm{v,rb}} = -\frac{G}{\hat{p}(\mathbf{x})} \cdot \mathrm{sat}\left(\frac{s}{\Phi}\right) \tag{38}$$

where Φ is the boundary layer thickness.

5 Experimental Results

Experiments were conducted to verify the aforementioned constant average pressure hypothesis, and demonstrate the performance of the pressure estimation algorithm and the corresponding robust force control approach. The experimental setup, which is shown schematically in Fig. 1, incorporated a double-acting pneumatic cylinder (0750D02-04A, Numatics, Novi, Michigan, USA) that was connected to a linear stage (Fig. 4). To limit the resulting motion to the allowable range, four extension springs (two on each side) were connected to the linear stage and functioned as the load of the actuator. The air flow to the actuator was controlled by a 4-way proportional control valve (MPYE-5-M5-010-B, FESTO, Germany), which features a position-controlled spool and a control bandwidth of 125 Hz. The system was supplied with compressed air at an absolute pressure of 653 kPa (94.7 psi), and the actuation force was measured with a tension/compression load cell mounted at the end of the piston rod (ELPF-T3E-100L, Measurement Specialties, Hampton, VA, USA). For the implementation of the control law, the system states as defined by (28) are required, including the pressures in the two cylinder chambers and the position and velocity of the piston. With the pressure estimation algorithm described in Section 2, the pressure sensors are not required for the implementation of the robust force controller. But in order to characterize the performance of the pressure estimation algorithm, a pair of pressure transducers (SDET-22T-D25-G14-U-M12, FESTO, Germany) were utilized to provide the measured values of the chamber pressures for the comparison purpose. In addition, a linear potentiometer (Midori model LP-100F) was utilized to measure the position (x), while the velocity ($\dot{x}$) was obtained via filtered differentiation of the measured position with a cut-off frequency at 25 Hz. The model and control parameters are listed in Table 1.

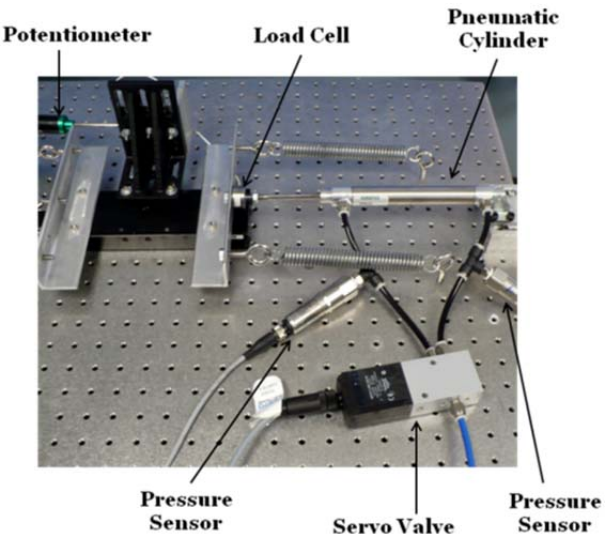

Fig. 4: *The experimental setup for the demonstration of the proposed pressure estimation algorithm and the corresponding robust controller*

The performances of the pressure estimation algorithm and the corresponding force controller were characterized in the tracking experiments of sinusoidal and square-wave functions. These experiments also served the purpose of testing the constant average pressure hypothesis as described in Section 2. In the experiments, the chamber pressures were measured with the aforementioned pressure sensors, and the average pressure was calculated based on the measured chamber pressures with Eq. (12). On the other hand, the estimated constant average pressure was also calculated based on the current supply pressure with Eq. (9), and compared with the measured average pressure. The typical results are shown in Fig. 5. As can be observed in these figures, the measured average pressure quickly rose to the level of steady state, and fluctuated only slightly afterwards. Furthermore, the difference between the measured and estimated average pressures is very small, which verifies the validity of the constant average pressure hypothesis in the real-life control applications.

Table 1: Model and controller parameters for experimental implementation of the proposed controller

Parameter	Description	Value	Unit
P_s	Supply pressure	653	kPa
P_{atm}	Atmosphere pressure	101	kPa
P_{ave}	Average pressure	460	kPa
A_a	Piston area facing Chamber *a*	285	mm^2
A_b	Piston area facing Chamber *b*	253	mm^2
A_r	Piston rod area	32	mm^2
L	Cylinder stroke	101.6	mm
γ	Ratio of specific heats	1.4	
R	Universal gas constant	0.287	kJ/kg·K
T	Gas temperature	293	K
C_f	Discharge coefficient	0.294	
C_r	Pressure ratio	0.528	
$A_{v,MAX}$	Maximum valve area	6.28	mm^2
G	Robustness gain	1.0×10^3	N/sec
Φ	Boundary layer width	0.5	N

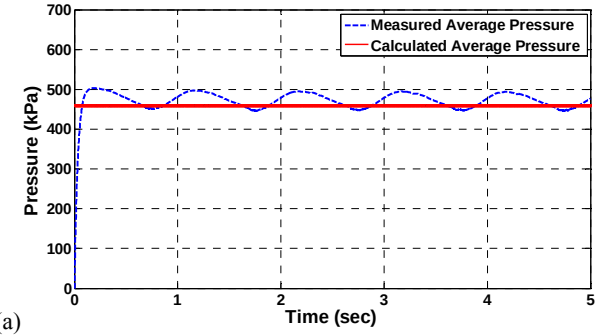

(a)

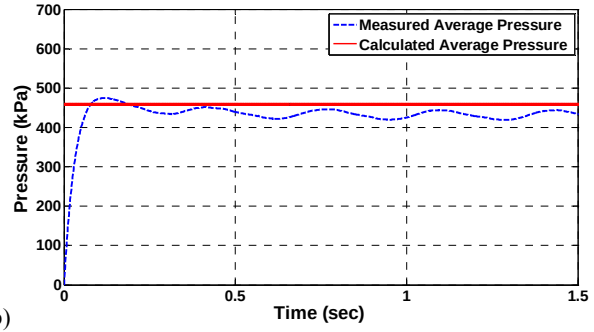

(b)

Fig. 5: *Comparison of the measured average pressure versus the constant average pressure calculated with (9) in 1.0 Hz sinusoidal tracking (a) and 3.0 Hz sinusoidal tracking (b)*

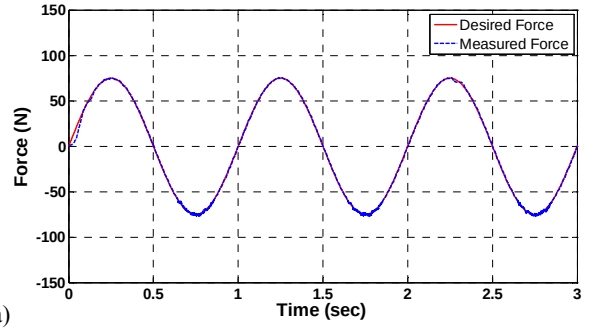

(a)

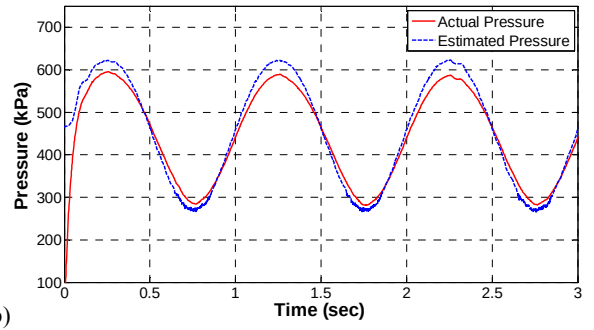

(b)

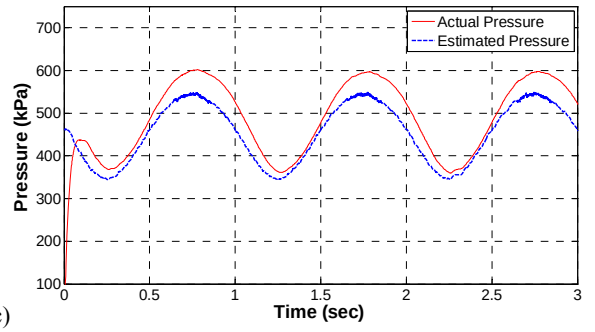

(c)

Fig. 6: *Force control performance (a) and the corresponding pressure estimation performances in Chamber a (b) and Chamber b (c) in the sinusoidal force tracking at 1.0 Hz*

The typical force tracking and pressure estimation performances are shown in Fig. 6 to 8. These results were obtained after repeated tuning of the robustness gain G. The robustness gain G determines the time needed to reach the sliding surface and the capability of tolerating model uncertainties and disturbances. Increasing G improves the tracking performance, but at the cost of more switching across the sliding surface. As such, a large of number G values have been experimentally tested to find

the optimal value that provides satisfactory control performance without causing excessive switching. As shown in Fig. 6a, 7a, and 8a, the actual force trajectory quickly converges to the desired force trajectory, displaying a fast dynamic response. Also, at steady state, the tracking error is very small, demonstrating the performance of the proposed robust force controller. In the corresponding pressure estimation performance plots (Fig. 6b, 6c, 7b, 7c, 8b, 8c), the estimated pressure curves also quickly converge to the measured pressure curves, with a very small amount of steady-state error. As demonstrated in these experiments, the pressure estimation algorithm is able to provide a high-quality pressure signal to support the implementation of the robust force controller. As such, the proposed control approach is able to enjoy the good control performance provided by the model-based control while eliminating the need for pressure sensors, which is highly useful for the reduction of cost and complexity of pneumatic actuation systems.

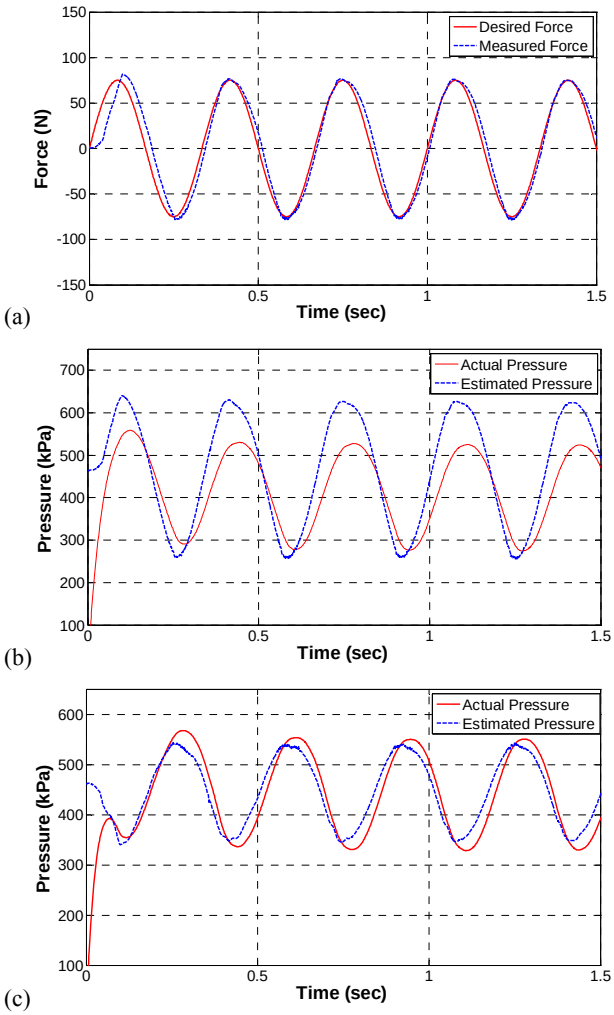

Fig. 7: *Force control performance (a) and the corresponding pressure estimation performances in Chamber a (b) and Chamber b (c) in the sinusoidal force tracking at 3.0 Hz*

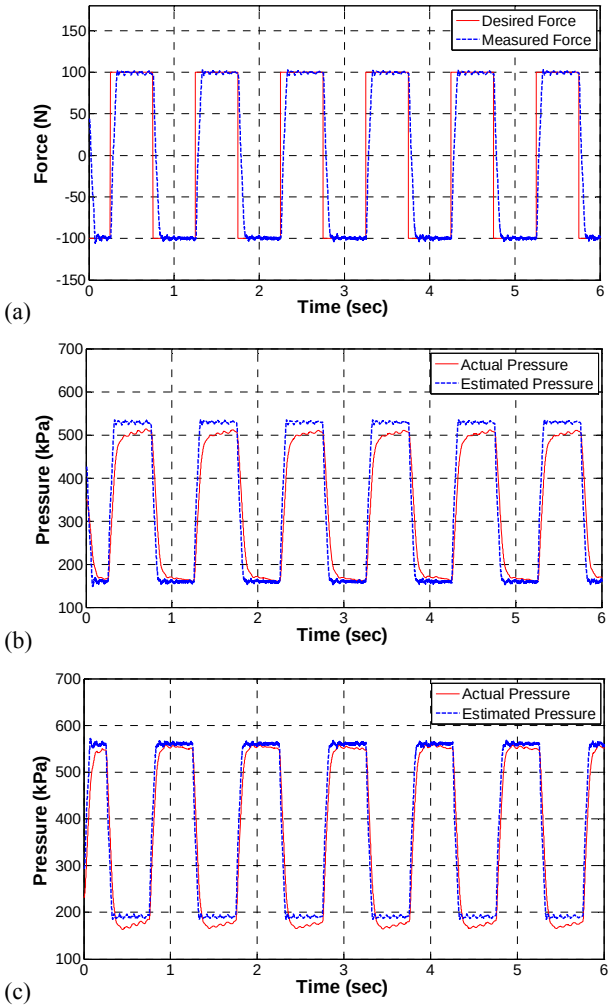

Fig. 8: *Force control performance (a) and the corresponding pressure estimation performances in Chamber a (b) and Chamber b (c) in the square-wave force tracking*

6 Conclusions

This paper presents a model-based robust force control approach for pneumatic actuation systems, which obtains the chamber pressure information through a unique pressure estimation algorithm In this algorithm, the average chamber pressure is assumed to be nearly constant, with the value determined based on the inflow-outflow balance of the actuator. The average pressure in the actuator, in combination with the measured actuation force, provides a set of simultaneous conditions to determine the two chamber pressures. Utilizing the estimated chamber pressures, a robust force control law was developed. As the basis of this controller, the dynamic model of the force-controlled pneumatic system was formulated first. Based on this nonlinear model, the standard sliding mode control approach was applied, providing robust control in the presence of model uncertainties and disturbances. Experimental results verified the hypothesis of constant average pressure, and demonstrated the effectiveness of the pressure estimation algorithm and the corresponding robust force control approach.

Nomenclature

A_a	Piston area facing Chamber a	[mm^2]
A_b	Piston area facing Chamber b	[mm^2]
A_r	Piston rod area	[mm^2]
A_v	Valve command	[mm^2]
$A_{v,e}$	Effective valve area	[mm^2]
$A_{v,eq}$	Equivalent control component	[mm^2]
$A_{v,in}$	Average valve area for pressurizing	[mm^2]
$A_{v,rb}$	Robustness control component	[mm^2]
$A_{v,out}$	Average valve area for depressurizing	[mm^2]
C_f	Discharge coefficient of the valve	[-]
C_r	Pressure ratio that divides the flow regimes into unchoked and choked flow through the orifice	[-]
F	Actuation force	[N]
F_d	Desired actuation force	[N]
G	Robustness gain	[N/sec]
γ	Ratio of specific heats	[-]
L	Cylinder stroke	[mm]
m_{in}	Cumulative inflow to the actuator	[kg]
$\dot{m}_{in,ave}$	Average inflow rate	[kg/s]
m_{out}	Cumulative outflow from the actuator	[kg]
$\dot{m}_{out,ave}$	Average outflow rate	[kg/s]
P_a	Absolute pressure in Chamber a	[kPa]
P_{atm}	Atmosphere pressure	[kPa]
P_{ave}	Average pressure in the actuator	[kPa]
P_b	Absolute pressure in Chamber b	[kPa]
P_d	Downstream pressure	[kPa]
Φ	Boundary layer width	[N]
P_s	Supply pressure	[kPa]
P_u	Upstream pressure	[kPa]
R	Universal gas constant	[kJ/kg·K]
T	Gas temperature	[K]
V_a	Volume of Chamber a	[mm^3]
V_b	Volume of Chamber b	[mm^3]
x	Piston displacement	[mm]

References

Arun, P. K., **Mishra, J. K.** and **Radke, M. G.** 1994. Reduced order sliding mode control for pneumatic actuator. *IEEE Transactions on Control System Technology*, vol. 2, no. 3, pp. 271 - 276.

Ben-Dov, D. and **Salcudean, S. E.** 1995. A force-controlled pneumatic actuator. *IEEE Transactions on Robotics and Automation*, vol. 11, no. 6, pp. 906 - 911.

Bigras, P. and **Khayati, K.** 2002. Nonlinear observer for pneumatic system with non negligible connection port restriction. *Proceedings of American Control Conference*, Anchorage, AK, pp. 3191-3195.

Blackburn, J. F., **Reethof, G.** and **Shearer, J. L.** 1960. *Fluid Power Control*, New York and London, Technology Press of M.I.T. and Wiley.

Bobrow, J. E. and **Jabbari, F.** 1991. Adaptive pneumatic force actuation and position control. *ASME Journal of Dynamic Systems, Measurement, and Control*, vol. 113, pp. 267 - 272.

Bregeault, V., **Plestan, F.**, **Shtessel, Y.** and **Poznyak, A.** 2010. Adaptive sliding mode control for an electropneumatic actuator. *2010 11th International Workshop on Variable Structure Systems*, pp. 260 - 265.

Girin, A., **Plestan, F.**, **Brun, X.**, **Glumineau, A.** and **Smaoui, M.** 2006. High gain and sliding mode observers for the control of an electropneumatic actuator. *Proceedings of the 2006 IEEE International Conference on Control Applications*, Munich, Germany, pp. 3128 - 3133.

Girin, A., **Plestan, F.**, **Brun, X.** and **Glumineau, A.** 2009. High-order sliding-mode controllers of an electropneumatic actuator: Application to an aeronautic benchmark. *IEEE Transactions on Control Systems Technology*, vol. 17, no. 3, pp. 633 - 645.

Gulati, N. and **Barth, E. J.** 2009. A globally stable, load-independent pressure observer for the servo control of pneumatic actuator. *IEEE/ASME Transactions on Mechatronics*, vol. 14, no. 3, pp. 295 -306.

Kazerooni, H. 2005. Design and analysis of pneumatic force generators for mobile robotic systems. *IEEE/ASME Transactions on Mechatronics*, vol. 10, no. 4, pp. 411 - 418.

Kuribayashi, K. 1992. Criteria for the evaluation of new actuators as energy converters. *Advanced Robotics*, vol. 7, no. 4, pp. 289 - 237.

McDonell, B. W., and **Bobrow, J. E.** 1993. Adaptive tracking control of an air powered robot actuator. *ASME Journal of Dynamic Systems, Measurement, and Control*, vol. 115, pp. 427 - 433.

Pandian, S. R., **Hayakawa, Y.**, **Kanazawa, Y.**, **Kamoyama, Y.** and **Kawamura, S.** 1997. Practical design of a sliding mode controller for pneumatic actuators. *ASME Journal of Dynamic Systems, Measurement, and Control*, vol. 119, no. 4, pp. 664 - 674.

Plestan, F., **Shtessel, Y.**, **Bregeault, V.** and **Poznyak, A.** 2010. Sliding mode control with gain adaptation – Application to an electropneumatic actuator. Control Engineering Practice, http://dx.doi.org/10.1016/j.conengprac.2012.04.012.

Richer, E. and **Hurmuzlu, Y.** 2000. A high performance pneumatic force actuator system: Part I-nonlinear mathematical model. *ASME Journal of Dynamic Systems, Measurement, and Control*, vol. 122, no. 3, pp. 416 - 425.

Richer, E. and **Hurmuzlu, Y.** 2000. A high performance pneumatic force actuator system: Part II-nonlinear control design. *ASME Journal of Dynamic Systems, Measurement, and Control*, vol. 122, no. 3, pp. 426 - 434.

Shearer, J. L. 1956. Study of pneumatic processes in the continuous control of motion with compressed air – I. *Transactions of the ASME*, vol. 78, pp. 233-242.

Shearer, J. L. 1956. Study of pneumatic processes in the continuous control of motion with compressed air – II. *Transactions of the ASME*, vol. 78, pp. 243 - 249.

Shearer, J. L. 1957. Nonlinear analog study of a high-pressure servomechanism. *Transactions of the ASME*, vol. 79, pp. 465 - 472.

Slotine, J. E. and **Li, Y.** 1991. *Applied Nonlinear Control*, Prentice Hall, New Jersey.

Smaoui, M., **Brun, X.** and **Thomasset, D.** 2006. A study on tracking position control of an electro-pneumatic system using backstepping design. *Control Engineering Practice*, vol. 14, pp. 923 - 933.

Smaoui, M., **Brun, X.** and **Thomasset, D.** 2008. High-order sliding mode for an electropneumatic system: A robust differentiator-controller design. *International Journal of Robust and Nonlinear Control*, vol. 18, pp. 481 - 501.

Taleb, M., **Levant, A.** and **Plestan, F.** 2012. Twisting algorithm adaptation for control of electropneumatic actuators. *12th IEEE Workshop on Variable Structure Systems*, pp. 178 - 183.

Tang, J. and **Walker, G.** 1995. Variable structure control of a pneumatic actuator. *ASME Journal of Dynamic Systems, Measurement, and Control*, vol. 117, pp. 88 - 92.

Wu, J., **Goldfarb, M.** and **Barth, E. J.** 2004. On the observability of pressure in a pneumatic servo actuator. *ASME Journal of Dynamic Systems, Measurement, and Control*, vol. 126, pp. 921 - 924.

Tad Driver
received his B.S. degree in mechanical engineering from Auburn University in 2007, and the M.S. and Ph.D. degrees in mechanical engineering from The University of Alabama in 2011 and 2012, respectively. While at The University of Alabama he performed research in the area of pneumatic actuator control and innovation, specifically that pertaining to pneumatic artificial muscles. His current research interests include applied nonlinear controls, biomechanics, and robotics.

Xiangrong Shen
is an assistant professor in the Department of Mechanical Engineering at the University of Alabama. He received his Ph.D. in Mechanical Engineering from Vanderbilt University in 2006, his M.S. in Mechanical Engineering from University of Nebraska - Lincoln in 2003, and his B.E. in Mechanical Engineering & Automation from Shanghai Jiao Tong University in 1998. Currently his research is focused on the design, modeling, and control of fluid power systems, as well as the application of fluid power actuation in biomedical robotic systems.